A composition density functional theory for mixtures based upon an infinitely polydisperse reference. II. Freezing in hard sphere mixtures

David A. Kofke[a] and Eduardo D. Glandt
Department of Chemical Engineering, University of Pennsylvania, Philadelphia, Pennsylvania 19104-6393

(Received 27 September 1989; accepted 11 December 1989)

A theory recently proposed by the authors [Kofke and Glandt, J. Chem. Phys. **92**, 658 (1990)] is applied to the study of freezing in hard spheres and hard sphere mixtures. The theory, which expresses the free energy of an arbitrary mixture as a functional of the composition density of an infinitely polydisperse (IP) reference, is used to evaluate the properties of mixtures of hard spheres constrained to the Wigner–Seitz cells of an fcc lattice. Semigrand Monte Carlo simulations are used to determine the properties of the IP reference mixture, which is also constrained to an fcc lattice. Freezing is determined by comparing the predicted properties of the Wigner–Seitz crystal with the known properties of the fluid phase. A freezing transition is found for monodisperse hard spheres; the estimated solid-phase density and the transition pressure differ from the accepted values by 2% and 8%, respectively. The treatment is also used to study freezing in polydisperse mixtures with Gaussian distributions of diameters. In accordance with the findings of others, an upper bound is found to the variance of the distribution, beyond which freezing no longer occurs. However, the maximum variance predicted here is approximately one order of magnitude less than that previously found. Discrepancies here and in the pure-fluid results are attributed largely to ergodic difficulties in the simulations of the IP reference. Finally, the possibility of a phase transition in IP mixtures is demonstrated through a calculation of the freezing point of IP hard spheres.

I. INTRODUCTION

In recent work,[1] we introduced the concept of an infinitely polydisperse mixture which, because it is characterized by a single length scale, exhibits many simplifying features. We then developed[2] a composition-space density functional theory for which infinitely polydisperse mixtures were shown to be a natural reference. The theory proved very effective when applied in test cases involving hard-sphere fluids in one and three dimensions. In the present work, we apply this new theory to the description of freezing in hard sphere mixtures.

The fluid–solid phase transition of hard spheres is a phenomenon of great theoretical importance. The fact that it even occurs was long uncertain, and it was only through the use of molecular simulation[3] that its presence was confirmed. Hard-sphere freezing is an appropriate model for crystallization in many systems, e.g., some types of colloidal suspensions.[4] Most attempts[5] at the development of theories which predict the freezing transition have met with little success. Recently, the field has seen a resurgence through the successful application of (configuration-space) density functional theory.[6] Haymet and co-workers[7,8] have extended this approach to the prediction of the freezing transition of hard-sphere mixtures and of polydisperse hard spheres. Unfortunately, there is very little controlled experimental data (i.e., Monte Carlo simulations) or alternative theoretical results with which to compare the predictions from these studies. Thus, because of the potential of yielding very useful results, and because infinitely polydisperse hard spheres are very easily characterized, we have chosen to further test the composition-space density functional theory by applying it to this problem.

Infinitely polydisperse substances are a class of mixtures in which the composition is described by a continuum and, for hard spheres, the configurational chemical potential distribution $\mu_c(\sigma)$ has a logarithmic dependence on the diameter σ

$$\beta\mu_c(\sigma) = \beta\mu_c(\sigma_o) + c_0 \ln \frac{\sigma}{\sigma_o}, \tag{1}$$

where σ_o is the diameter of an arbitrary reference component, and $\beta = 1/k_B T$ with T the absolute temperature and k_B Boltzmann's constant. The dimensionless parameter c_0 characterizes the distribution. Equation (1) provides a semigrand representation[9,10] of the mixture, in which the composition is specified indirectly via the distribution of chemical potential differences. Mixtures described by this distribution are termed[1] "infinitely polydisperse" because Eq. (1) does not explicitly impose any limits on particle size; instead, the diameters are limited intrinsically, by packing restraints. Indeed, Eq. (1) introduces no characteristic length scales whatsoever. As a consequence, a simple—and sometimes analytic—representation of many properties can be obtained. Dimensioned quantities such as the pressure and the composition can only be reduced by the density, which provides the single independent characteristic length scale. When expressed in reduced form, these properties become independent of the density. In particular, the equation of state can be determined exactly, and is given by

$$Z \equiv \frac{\beta P}{\rho} = \frac{4 + c_0}{3}. \tag{2}$$

Although the reference chemical potential $\mu(\sigma_o)$ cannot, in

[a] Present address: Department of Chemical Engineering, SUNY at Buffalo, Buffalo, New York 14620.

 0021-9606/90/074417-09$03.00

general, also be determined analytically, its variation with the density is simply expressed

$$\beta\mu_c(\sigma_o) = \ln[\rho^{4/3}K(c_0)] + c_0 \ln[\rho^{1/3}\sigma_o], \quad (3)$$

where the dimensionless quantity $K(c_0)$ is independent of density. Also, while the composition is not given *a priori*, it too has a simple density dependence

$$p(\sigma) = \rho^{1/3}p^*(\sigma^*), \quad (4)$$

where $\sigma^* \equiv \rho^{1/3}\sigma$ and p^* is otherwise independent of density. For hard spheres, an accurate approximation for the composition can be derived using the Percus–Yevick theory

$$p(\sigma) = \rho^{1/3}(\rho^{1/3}\sigma)^{c_0} \exp[b_0 + b_1\sigma + b_2\sigma^2 + b_3\sigma^3] \quad (5)$$

which may be expressed in an alternate, dimensionless form

$$p^*(\sigma) = (Z^{1/3}\sigma^*)^{c_0} \exp[b_0^* + b_1^*(Z^{1/3}\sigma^*) + b_2^*(Z^{1/3}\sigma^*)^2 + b_3^*(Z^{1/3}\sigma^*)^3], \quad (6)$$

where the compressibility factor Z is given in terms of c_0 by Eq. (2). The coefficients b_0^*, b_1^*, b_2^*, and b_3^* are dimensionless and invariant with density, although they do depend on c_0. By choosing to include Z in the dimensionless expression for the composition, we have reduced the b's by the pressure βP rather than the density [i.e., $b_n^* = b_n/(\beta P)^{n/3}$]. This approach is advantageous because it simplifies the dependence of the coefficients on c_0, as demonstrated in Fig. 1, where b_1^*, b_2^*, and b_3^*, are plotted. Remarkably, the coefficient b_3 is virtually independent of c_0. This observation can be explained using scaled-particle theory,[11] which predicts a constant b_3 of $-\pi/6$ for all c_0.[10] The coefficients in Fig. 1 were determined from an empirical Carnahan–Starling[12]-type combination of the Percus–Yevick virial and compressibility equations of state.[13] Since scaled particle theory produces an equation of state identical to the Percus–Yevick compressibility result, the compressibility equation of state should also produce a constant b_3^*. It is interesting to see that the semiempirical result displays nearly the same behavior.

A key result form the composition-space density functional theory[2] is an expression for the semigrand free energy functional Y in terms of the chemical potential difference distribution $\beta\Delta\mu[=\beta\mu(\sigma) - \beta\mu(\sigma_o)]$ and the free energy of a reference mixture characterized by $\beta\Delta\mu_o$ and of known composition $p_o(\sigma)$

$$Y[\beta\Delta\mu] = Y[\beta\Delta\mu_o] - N\ln\int P_o(\sigma)\exp[\beta\Delta\mu_c(\sigma) - \beta\Delta\mu_{co}(\sigma)]d\sigma. \quad (7)$$

Simple expressions can be derived from Eq. (7) which relate the thermodynamic properties of the mixture of interest directly to its composition $p(\sigma)$ (rather than to $\beta\Delta\mu$). The success of the theory hinges on the proper selection of the reference mixture. For an infinitely polydisperse reference, the only degree of freedom for making this choice is in the parameter c_0. It can be deduced[2] from Eq. (7) that if c_0 satisfies

$$\int p(\sigma)\left\{1 + \sigma^*\frac{d}{d\sigma^*}\ln[p_o^*(\sigma^*;c_0)]\right\}d\sigma = 0 \quad (8)$$

then the compressibility factor and the chemical potential distribution of the mixture are given by

$$Z = Z_o = \frac{4 + c_0}{3} \quad (9)$$

$$\beta\mu_c(\sigma) = \beta\mu_{co}(\sigma) + \ln\frac{p(\sigma)}{p_o(\sigma)} + (Z - Z_o). \quad (10)$$

With the reference composition p_0^* given by Eq. (6), Eq. (8) becomes

$$1 + c_0 + b_1^*Z_o^{1/3}s_1^* + b_2^*Z_o^{2/3}s_2^* + b_3^*Z_o s_3^* = 0, \quad (11)$$

where s_n^* is the nth moment—about the origin—of the composition of the mixture of interest $p(\sigma)$ reduced by the density: $s_n^* = \rho^{n/3}s_n$. Given the coefficients b_1^*, b_2^*, and b_3^* as a function of c_0, and given the density and composition of the mixture of interest, Eq. (11) may be solved for the optimal c_0. The thermodynamic properties then follow directly from Eqs. (7), (9), and (10). Alternatively, if one is mapping out the entire equation of state, it is simpler to specify Z (and therefore c_0 and the b^*'s) first, and then solve Eq. (11) for the density, which is simply a cubic in $\rho^{1/3}$.

In order to apply this theory to the study of freezing in hard spheres, it is necessary to determine, as a function of c_0, the composition of infinitely polydisperse spheres in the crystalline state. The most direct way to evaluate these distributions is by Monte Carlo simulation. The methods for performing and evaluating the results of these simulations are described in Sec. II. The results themselves are reported in Sec. III. In Sec. IV, the simulation results are introduced into the theory, and a description of freezing in single component hard spheres and in hard-sphere mixtures with Gaussian compositions is attempted. The intriguing possibility of phase transitions in infinitely polydisperse mixtures is briefly considered in Sec. V, and conclusions are summarized in Sec. VI.

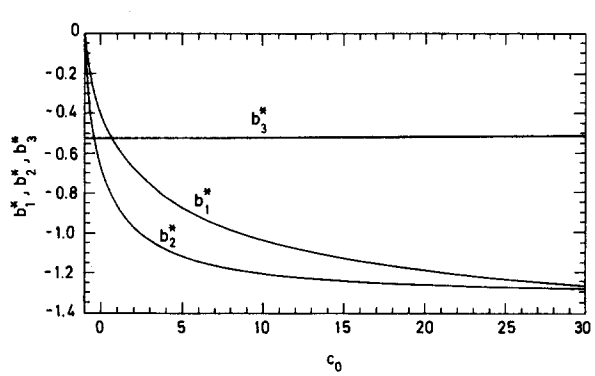

FIG. 1. Density-invariant composition coefficients b_1^*, b_2^*, and b_3^* as a function of the $\Delta\mu$ parameter c_0. The composition of an infinitely polydisperse mixture of hard spheres is given in terms of these coefficients and c_0 according to Eq. (6).

II. METHODOLOGY

A. Description of the fluid–solid transition

The effect of increasing c_0 for an infinitely polydisperse hard sphere mixture is to give preference to spheres of larger diameter, and thus to increase the total volume occupied by

the spheres. Thus, as one would expect, the optimal c_0 of an infinitely polydisperse reference which corresponds to a crystalline hard-sphere mixture is relatively large. For example, the freezing transition for pure hard spheres occurs when the compressibility factor in the crystal is about 11, which corresponds [via Eq. (2)] to a c_0 of nearly 30.

To evaluate the properties of the infinitely polydisperse hard sphere system at such high c_0, and thus at high packing fraction, we have adopted a method similar to that used by Hoover and Ree[3] in their pioneering work on the freezing of pure hard spheres. In their approach, simulations were performed of hard spheres constrained to the Wigner–Seitz cells of a face-centered cubic (fcc) lattice, with one particle per cell. Results from simulations at various densities yielded an equation of state for the single-occupancy system, which was then integrated from low density—where the chemical potential could be estimated analytically—to densities typical of the solid phase. This yielded the chemical potential as a function of density. At high enough density, the single-occupancy system cannot be distinguished from the hard-sphere crystal. This was confirmed by the simulations, in which the constraints were never invoked above a certain density, lower than that computed for the freezing transition. The transition was determined when the chemical potential of a particle in the constrained system was equal that in a fluid at the same pressure (or, equivalently, when the entropies were equal).

In applying the method of Hoover and Ree to infinitely polydisperse mixtures, the parameter c_0 plays a role analogous to that of the density for a pure fluid. For c_0 sufficiently large, a crystalline phase is likely to become more stable than the fluid, and thus in this regime it is appropriate to use a single-occupancy model. As in the application to fluid mixtures,[2] the required input to the theory is the density-invariant infinitely polydisperse composition, but for a single-occupancy mixture instead of an unconstrained mixture; these distributions are straightforward to evaluate by Monte Carlo simulation. However, it is also necessary to know—as a function of c_0—the reference-component chemical potential or, equivalently, the parameter K in Eq. (3). In analogy to the method of Hoover and Ree, this quantity can be computed by integration of a series of simulation results—for increasing c_0—performed for a single-occupancy, infinitely polydisperse, hard sphere system. Specifically, the semigrand fundamental equation[9,10] is integrated from state a to state b at constant temperature and density to yield the necessary relation

$$\ln K(c_0^b) = \ln K(c_0^a) + (Z^b - Z^a) - \int_{c_0^a}^{c_0^b} s_0^*(\hat{c}_0)\,d\hat{c}_0\,, \tag{12}$$

where s_0^* is the dimensionless log moment of the composition distribution

$$s_0^* = \int_0^\infty \ln(\rho^{1/3}\sigma)p(\sigma)\,d\sigma \tag{13}$$

and is easily obtained from the simulations. The integral in Eq. (12) is more easily evaluated if it is recognized that s_0^* diverges asymptotically as $1/(1+c_0)$ when $c_0 \to -1$ (this result is developed in the Appendix). Thus, by defining a reduced K, κ, according to

$$K = (1+c_0)\kappa\,, \tag{14}$$

Eq. (12) can be expressed in terms of quantities which are finite over the entire range of c_0

$$\ln\kappa(c_0^b) = \ln\kappa(c_0^a) + \tfrac{1}{3}(c_0^b - c_0^a) - \int_{c_0^a}^{c_0^b}\left[s_0^*(\hat{c}_0) + \frac{1}{1+\hat{c}_0}\right]d\hat{c}_0\,, \tag{15}$$

where Eq. (2) has been used to substitute for $Z^b - Z^a$. As $c_0 \to -1$, $\ln\kappa$ vanishes for an unconstrained hard-sphere fluid, while it approaches unity for a single-occupancy system. This difference is a manifestation of the so-called "communal entropy" ΔS_c.[3] For an ideal gas ($c_0 = -1$), $\Delta S_c = Nk_B$, while at high packing fractions (large c_0), $\Delta S_c = 0$. Insertion of this limiting behavior into Eq. (15) yields the final working equation for κ

$$\ln\kappa(c_0) = 1 + \tfrac{1}{3}(c_0+1) - \int_{-1}^{c_0}\left[s_0^*(\hat{c}_0) + \frac{1}{1+\hat{c}_0}\right]d\hat{c}_0 \tag{16}$$

With this description of $\beta\mu(\sigma;c_0)$, and with the compositions obtained directly from the simulations, the perturbation theory may be applied to estimate the properties of a single-occupancy system of *any* composition. By combining these predictions with the known properties of the fluid phase, the fluid–solid transition can be located.

B. Simulation details

We performed a series of simulations of single-occupancy, infinitely polydisperse hard spheres in the isobaric semigrand ensemble, with values of the parameter c_0 ranging from -0.9 to 56. The standard Monte Carlo method for this ensemble[10] was implemented as follows. A particle was chosen at random. With equal probability, it was either displaced randomly, or its diameter was increased or decreased by a random amount. If the perturbation resulted in overlap with another particle, the new configuration was rejected. Otherwise, if the change was a displacement, and if the particle had not left its unit cell,[14] the move was accepted immediately. In the case of a size change, the new configuration was accepted with probability $(\sigma_{\text{new}}/\sigma_{\text{old}})^{c_0}$, where σ_{old} and σ_{new} are the old and new diameters, respectively. After every ten attempted particle perturbations, the system volume was changed by a random amount, and all particle separations were scaled up or down accordingly. If this resulted in no particle overlap, the change was accepted with probability $\exp[N\ln(V_{\text{new}}/V_{\text{old}}) - \beta P(V_{\text{new}} - V_{\text{old}})]$, where N is the number of particles used in the simulation, and V_{old} and V_{new} are the old and new volumes, respectively. Maximum allowable displacements (ten values, each optimized for a different range of diameters) and maximum size and volume changes were independently adjusted to result in a 50% acceptance rate.

Convergence of the simulations was enhanced, and some ergodic difficulties were overcome, through the use of an algorithm which combined this standard Monte Carlo method with analytic integration over some of the degrees of freedom. The fcc lattice can be decomposed into four simple-cubic (sc) sublattices. The integrations *over the species identities* of the particles occupying half of one of these sublattices were performed analytically. This subset of the spheres represents the largest group which can be selected such that its members do not interact with one another (they are fourth-nearest neighbors). For a given configuration, each particle in this subset contributes an amount $D_j = \sigma_{m,j}{}^{(c_0+1)}/(c_0+1)$ to the partition function, where $\sigma_{m,j}$ is maximum allowable diameter for particle j—that which first results in overlap of j with another (regular) particle. The particles in the subset were displaced just as the other hard spheres, but of course they did not randomly explore diameters. To account for their presence, the probability of acceptance of any perturbation was modified by multiplying it by the product $\Pi_j\ (D_{\text{new}}/D_{\text{old}})_j$, which was taken over all members of the subset affected by the change. This approach is reminiscent of that employed by Wood,[15] who used analytic integration of the volume in isobaric simulations of hard spheres.

The composition was tabulated, and separate averages were also recorded for several of its moments [including the log moment, given by Eq. (13)]. Three independent averages of the composition and its moments were taken, corresponding to the three types of lattice sites: the analytically integrated subset, those which share the sc lattice with the subset, and all of the sites on the remaining three sc lattices. Reported values represent the mean of the three averages, weighted according to the number of particles represented by each. The average compositions for the three types of sites did not differ significantly from one another.

The isobaric ensemble was chosen because it allows for simple application of Eq. (2) as a consistency check for the simulation. In each simulation, the pressure was selected to result in a density of unity: $\beta P = (4 + c_0)/3$. Thus, a simple examination of the volume average provided a check of the accuracy of the algorithm and the convergence of the simulations. In all but one case, the average volume was well within a few percent of the required value. Nevertheless, all quantities reported here and used in subsequent calculations were reduced by the average simulation density. Not doing so (i.e., assuming a density of unity) significantly increased the scatter in the data.

A total of 76 simulations were performed. Most of the simulations were carried out with 256 particles, and equivalent results were found in a few simulations of 500 particles. Typically, 2×10^6 configurations were sampled, including about 0.5×10^6 which were dropped to allow equilibration, although some simulations sampled as many as 8×10^6 configurations. Errors in the simulation averages were estimated using the method of Kolafa.[16] Only second-nearest neighbor interactions were considered; again, a few simulations which accounted for more distant interactions produced identical results. Further details are provided elsewhere.[10]

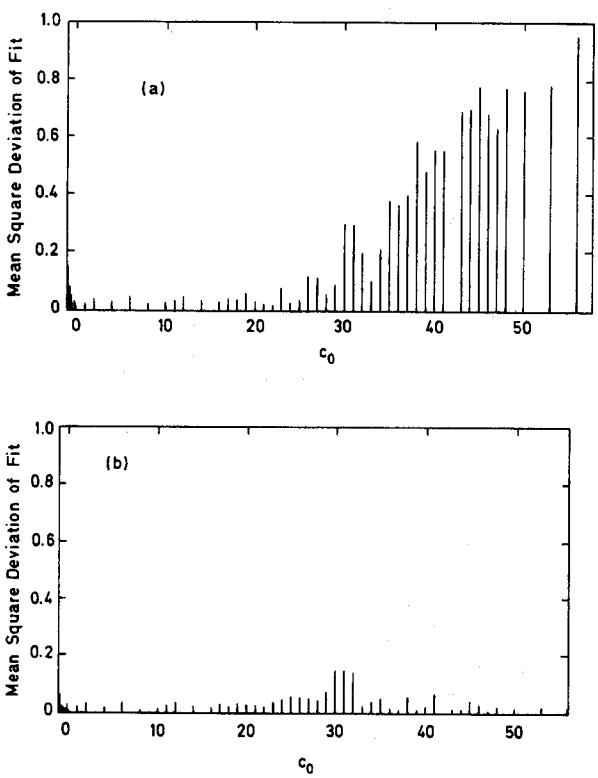

FIG. 2. Description of the goodness of the fit of the simulated compositions (a) when the b parameters are given by Eqs. (17) for all c_0; and (b) when the b parameters are given by Eqs. (17) for $c_0 < 31$ and by Eqs. (20) for $c_0 \geqslant 31$. Plotted is the summand of Eq. (18) as a function of the $\Delta\mu$ parameter c_0. A larger value indicates a poorer fit of the composition.

III. RESULTS

In order to present the results in a form suitable for use by others, the average compositions from the single-occupancy simulations were fit to empirical expressions that are explicit in c_0 and σ. The form chosen for the fitting functions was based upon the behavior of the fluid-phase compositions, as reviewed in the Sec. I. This approach relies upon the reasonable assumption that, as least for small c_0, the difference in behavior between fluid and single-occupancy hard spheres is more quantitative than qualitative. Therefore, Eq. (6) was used to describe the σ dependence of the composition, and, as suggested by Fig. 1, the b^* parameters were given by the following functions of c_0:

$$b_1^* = \frac{b_{11}(1+c_0)}{[1+b_{12}^2(1+c_0)]}, \tag{17a}$$

$$b_2^* = \frac{b_{21}(1+c_0)}{[1+b_{22}^2(1+c_0)]}, \tag{17b}$$

$$b_3^* = b_{31} + b_{32}(1+c_0)\,. \tag{17c}$$

These equations introduce six empirical parameters: b_{11}, b_{12}, b_{21}, b_{22}, b_{31}, and b_{32}; the quantity b_0^* is determined by normalization of the composition. In order to perform the nonlinear least-squares fit without *a priori* knowledge of b_0^*, the objective function Ω for minimization was selected as follows

$$\Omega = \sum_{c_0} [\ \overline{(\Delta y)^2} - \overline{\Delta y}^2\ ] , \tag{18}$$

where

$$\Delta y = y_{\text{sim}} - y_{\text{fit}}$$

with

$$y_{\text{sim}} = \ln[p^*_{\text{sim}}(\sigma^*)] - c_0 \ln \sigma^* ,$$

$$y_{\text{fit}} = b_1^*(Z^{1/3}\sigma^*) + b_2^*(Z^{1/3}\sigma^*)^2 + b_3^*(Z^{1/3}\sigma^*)^3 ,$$

with b_1^*, b_2^*, and b_3^*, given by Eq. (17), and Z by Eq. (2); the subscript sim indicates a simulation result. The overbars in Eq. (18) indicate an average over diameters, weighted according to the estimated error δp in the simulated composition

$$\overline{[\cdots]} = \sum_{\sigma} w(\sigma)[\cdots]$$

$$w(\sigma^*) \propto p^*(\sigma^*)/\delta p(\sigma^*); \quad \sum_{\sigma} w(\sigma^*) = 1 . \tag{19}$$

In Fig. 2(a), the mean square deviation of the fit—the summand of Eq. (18)—is plotted against c_0. It is seen that the fit rapidly deteriorates for c_0 greater than about 30. This observation suggests that a substantial improvement can be achieved by introducing a different functional form for $b^*(c_0)$ for $c_0 > 30$. A simple cubic in c_0 was chosen for this regime, thus

$$b_1^* = B_{10} + B_{11}(c_0 - c_0^{\text{cut}}) + B_{12}(c_0 - c_0^{\text{cut}})^2 + B_{13}(c_0 - c_0^{\text{cut}})^3 , \tag{20a}$$

$$b_2^* = B_{20} + B_{21}(c_0 - c_0^{\text{cut}}) + B_{22}(c_0 - c_0^{\text{cut}})^2 + B_{23}(c_0 - c_0^{\text{cut}})^3 , \tag{20b}$$

$$b_3^* = B_{30} + B_{31}(c_0 - c_0^{\text{cut}}) + B_{32}(c_0 - c_0^{\text{cut}})^2 + B_{33}(c_0 - c_0^{\text{cut}})^3 , \tag{20c}$$

with the coefficients B_{10}, B_{20}, and B_{30} selected to maintain continuity of the b^*'s; c_0^{cut} is the value of c_0 in which the fit changes from Eqs. (17) to Eqs. (20). With Eqs. (20), the minimization of Ω may be solved directly rather than numerically. The coefficients b_{ij} and B_{ij} which minimize Ω are listed in Table I (note that b_3^* is again virtually independent of c_0 for $c_0 < c_0^{\text{cut}}$); an optimum in c_0^{cut} was found at $c_0^{\text{cut}} = 31$. As seen in Fig. 2(b), this modification does indeed result in a greatly improved fit of the composition. In Figs. 3 and 4 some moments of the fitted composition are compared with the moments computed directly in the simulation.

Given this explicit representation of the composition, it is a simple matter to compute numerically the log moment s_0^* needed to evaluate the chemical potential coefficient κ. Note that when $c_0 < 0$ some care must be exercised to remove the singularity at zero diameter before performing the quadrature. The "excess" log moment $[s_0^* + 1/(1 + c_0)]$ is displayed in Fig. 4 (note that this quantity does not vanish at $c_0 = -1$). It may be numerically integrated according to Eq. (16) to yield κ as a function of c_0; the result is plotted in Fig. 5.

TABLE I. Coefficients determined from fitting the simulation compositions according to Eqs. (17) and (20).

	$c_0 < 31$ [Eqs. (17a)–(17c)]			
	n			
	1		2	
b_{1n}	2.130		3.420	
b_{2n}	−1.371		0.9645	
b_{3n}	−0.6686		0.004 556	
	$c_0 \geqslant 31$ [Eqs. (20a)–(20c)]			
	n			
	0	1	2	3
B_{1n}	0.181 71	−5.7221	−0.016 333	−0.018 378
B_{2n}	−1.4262	4.1093	−0.053 350	0.006 9142
B_{3n}	−0.522 81	−0.827 98	0.020 822	−0.001 0043

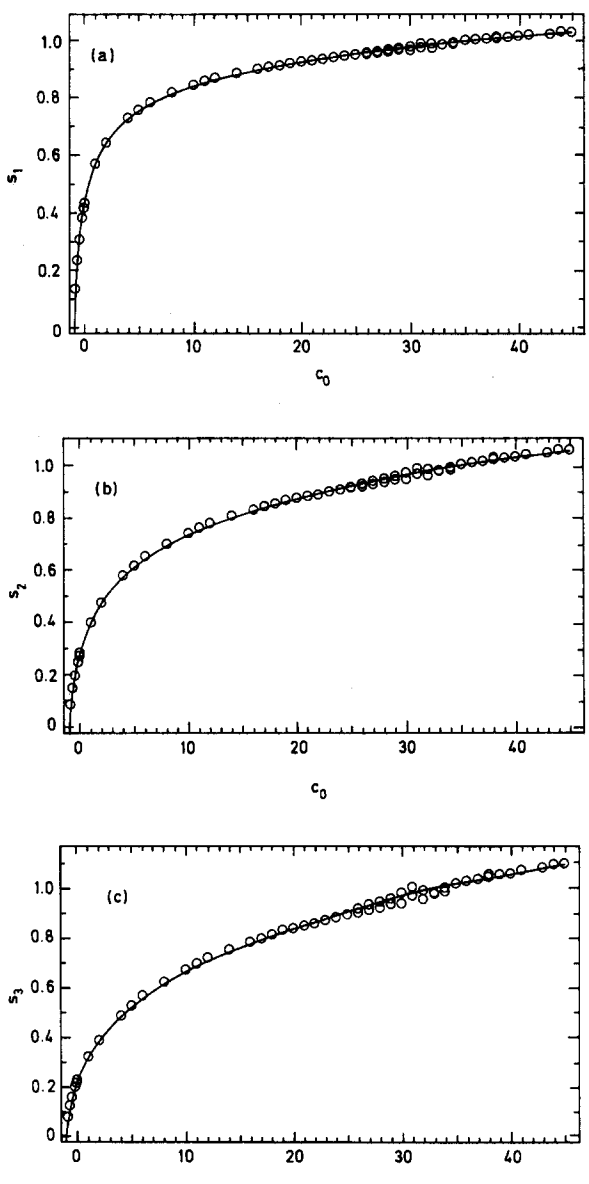

FIG. 3. Comparison of the moments of the composition as determined directly from the simulations (circles) with those computed from the fitted compositions (solid line). Plotted are (a) the first moment; (b) the second moment; and (c) the third moment about the origin.

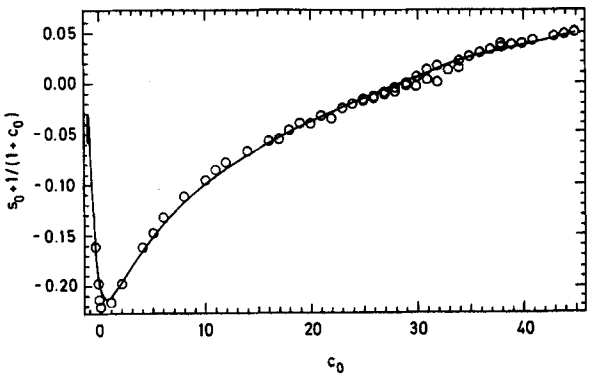

FIG. 4. Log moment of the composition, defined in Eq. (13), adjusted to remove the singularity at $c_0 = -1$. Shown are values determined directly from the simulations (circles) and values computed from the fit of the compositions (solid line). Simulation values (circles) at $c_0 = -0.9$ and -0.7 are off of the scale (having values of about 4.0) and are likely to be incorrect due to errors in estimating them directly from the simulations.

IV. APPLICATION OF THEORY

A. Pure hard spheres

The simulation results were first input to the perturbation theory to predict the phase diagram for *monodisperse* hard spheres, because this case is very well documented. The results are plotted in Fig. 6. Here are shown the equation of state for the pure fluid (according to the equation of Carnahan and Starling[12]), the results of Hoover and Ree for the single-occupancy system[3] (and extended using the equation of state for the solid of Hall[17]), and the single-occupancy predictions of the proposed theory. In Fig. 6(a), the compressibility factor $\beta P/\rho$ is plotted, while in Fig. 6(b) the pressure βP is plotted and the freezing transition is indicated.

The perturbation theory performs remarkably well, but only below a certain density. The results of Hoover and Ree suggest a cusp in the single-occupancy isotherm at a 60% expansion from close packing. Hoover and Ree report that the cusp occurs at the density at which the lattice constraint begins to be unnecessary to hold the crystal together, and therefore it represents the point at which the solid becomes mechanically stable. The isotherm from the perturbation theory does not display this behavior, and continues smoothly through the cusp density, asymptotically reapproaching

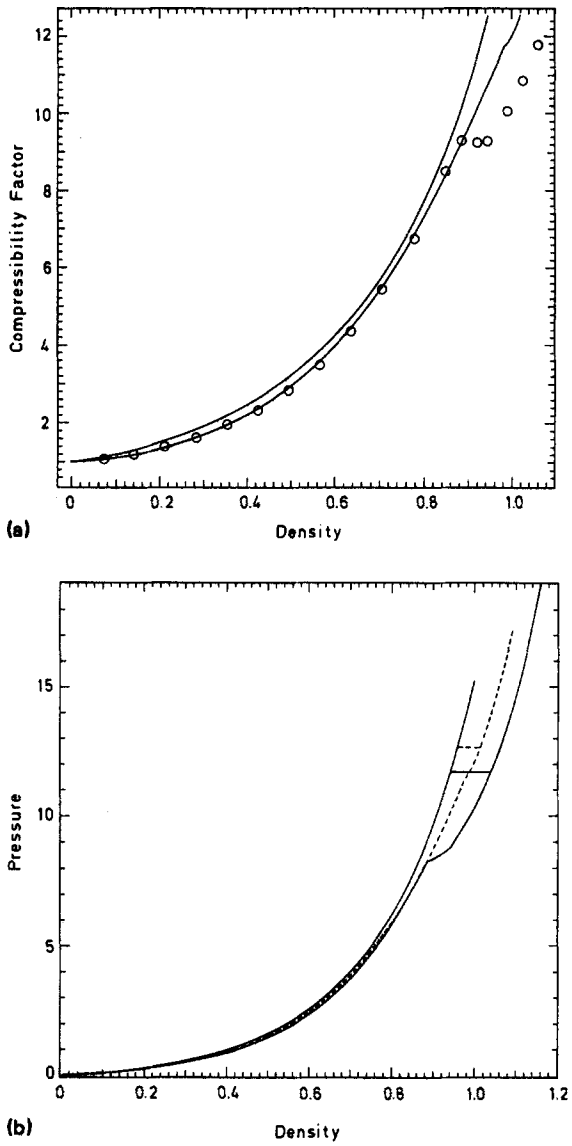

FIG. 6. (a) Compressibility factor for pure hard spheres. The upper solid line represents the fluid-phase equation of state of Carnahan and Starling (Ref. 12), the circles are the accurate fcc single-occupancy results of Hoover and Ree (Ref. 3); the lower line represents the single occupancy results predicted from the theory. (b) Freezing transition in pure hard spheres. The solid lines represent the literature results for the fluid (Ref. 12) and single-occupancy fcc crystal (Refs. 3, 17), and the broken line is the single-occupancy isotherm predicted from the theory. The horizontal lines connecting the fluid- and crystal-phase isotherms indicate the freezing transition.

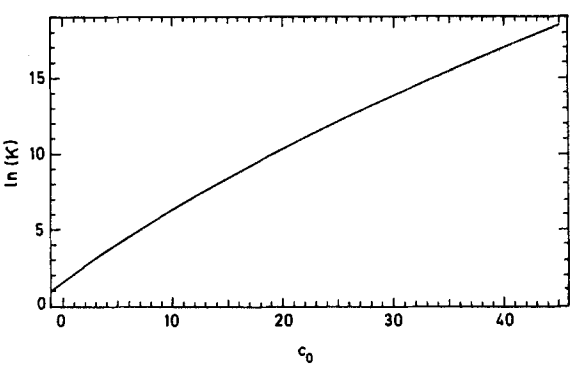

FIG. 5. Reduced, density-invariant chemical potential coefficient κ, defined in Eq. (14), plotted as a function of the $\Delta\mu$ parameter c_0.

the correct solid-phase curve. It is likely that the source of this discrepancy is the existence of a separate crystalline phase in the infinitely polydisperse mixture, one which allows better packing of the hard spheres in the fcc crystal. Tighter packing could be achieved through spatial ordering of the particles according to their average diameters. For a systems where the particles can readjust their diameters such an ordered phase may become thermodynamically favorable at large c_0, just as the pure crystal is favored at high density. In the simulation of a fluid under compression one does not expect to observe spontaneous crystallization; similarly, we could not hope for a substitutionally disordered fcc mixture to become ordered spontaneously. However, in an

extension of the single-occupancy approach, appropriate diameter-position correlations could be *imposed* in the infinitely polydisperse crystal. Such an approach would allow comparison of the relative stability of the highly ordered system with the substitutionally disordered crystal studied here. Of course, the challenge in such an undertaking is in determining the form of the added constraints. This will be left for future work.

Despite the discrepancies between these results and the correct behavior, the perturbation theory does predict a fluid–solid phase transition. The prediction is shown in Fig. 6(b), along with the correct transition, by a horizontal line. The predicted pressure at the transition is 12.62, and the densities of the equilibrium fluid and solid phases are 0.958 and 1.015, respectively.

B. Mixtures with Gaussian distributions of diameters

McRae and Haymet[8] have applied density functional theory to the study of freezing in polydisperse hard-sphere mixtures, with Gaussian distributions of diameters. Systems exhibiting polydispersity often have very narrow composition distributions, and are well modeled by a Gaussian form. For "wide" distributions, covering a large range of diameters, it can be reasoned that the freezing transition does not occur. Indeed, McRae and Haymet report that when the standard deviation of the particle size distribution exceeds approximately 5% of the mean size, the liquid no longer freezes into a crystalline array. Thus, the required wide distributions are actually quite narrow. Also, McRae and Haymet find that the density difference between the two phases—the order parameter for the transition—does not approach zero at the critical polydispersity, but instead remains finite while the transition abruptly disappears. We have applied the proposed theory to this system, and find the same qualitative results.

In the calculations reported here, a Gaussian composition of variance η^2 was first chosen for the solid phase. An approximation was then introduced: the fluid-phase composition was also constrained to a Gaussian form, but with a mean and variance determined by the requirements of phase equilibrium—equality of pressure and of chemical potential distributions. This is a reasonable approximation. When the perturbation theory is applied to the Gaussian solid, the composition of the fluid in equilibrium with it has the form of Eq. (5), with $c_0 = 0$. However, it is found that the coefficient b_3 (which should be negative) is often very small compared to b_1 and to b_2 (which is negative). Sometimes b_3 is even positive, an unreasonable finding which results from neglecting small higher order terms, b_4, b_5, etc. Since b_3 is itself small, it can be safely neglected altogether, with the net effect of constraining the fluid phase composition to a Gaussian form. This is a weaker assumption than the "constrained eutectic" used by McRae and Haymet, and which is further discussed below.

In Fig. 6 are plotted the equilibrium fluid and solid densities, according to the proposed theory, as a function of the standard deviation η of the composition distribution of the solid phase. The freezing transition abruptly disappears above a certain polydispersity, which is found here to be

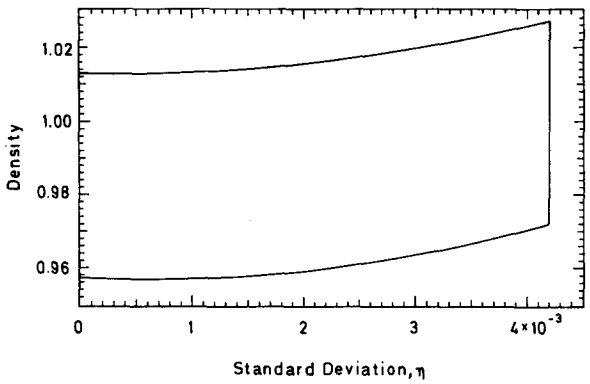

FIG. 7. Phase diagram for a mixture of hard spheres. The solid-phase composition is Gaussian, with variance η^2; the fluid-phase composition is constrained to a Gaussian form, with mean and variance determined by the requirements of phase equilibrium. No transition is found for $\eta > 0.0042$.

$\eta = 0.003$. This critical polydispersity is about at order of magnitude lower than that found by McRae and Haymet. There are several possible reasons for this large discrepancy. Part is certainly due to systemtic errors in the simulated infinitely polydisperse compositions, which were shown above to lead to an inaccurate pure-fluid freezing transition. Indeed, the calculations here predict an increase with η of the fractional density change upon freezing, which is unlikely to be correct. Another contributing source of discrepancy is possibly the constrained eutectic assumption used by McRae and Haymet, in which the compositions of the two phases were forced to be equal. This constraint was imposed in lieu of the rigorously correct equality of the chemical potential difference distributions, which was followed more closely in the calculations reported here. Constrained eutectic calculations were also performed here using the proposed theory, with vastly different, somewhat unphysical results. Again, an upper polydispersity limit to freezing was found, but it occurred at much larger polydispersities, $\eta = 0.18$, at a point where the solid-phase equilibrium density had fallen below that of the fluid. Further examination of the constrained eutectic approximation is clearly warranted.

V. PHASE TRANSITIONS IN INFINITELY POLYDISPERSE FLUIDS

Finally, we briefly consider the interesting situation in which two infinitely polydisperse mixtures are in thermodynamic equilibrium. Here, equality of all chemical potentials implies that c_0 must be the same in both phases. From Eq. (2) it then follows that the compressibility factors must also be equal. Moreover, equality of pressures leads us to rigorously conclude that the (number) densities must also be equal. The two phases can only differ in their compositions.

Using the single-occupancy simulation results described above, along with the equation of state of Mansoori *et al.*[13] for the fluid phase, it was possible to determine a freezing transition in the infinitely polydisperse hard-sphere fluid. The chemical potential of the reference component in the fluid and crystalline phases is plotted in Fig. 8 as a function of c_0. The curves cross, indicating a phase transition, at $c_0 = 40.5$. The variances of the fluid- and solid-phase com-

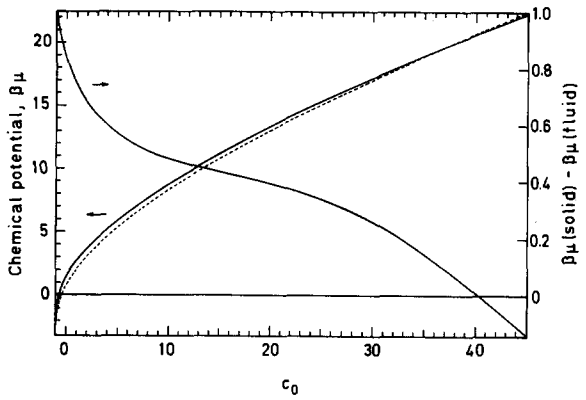

FIG. 8. Freezing in infinitely polydisperse hard spheres. On the left scale, the solid and dashed lines represent the chemical potential of an arbitrary component in the solid and fluid phases, respectively. On the right scale is plotted the difference in these chemical potentials. The freezing transition occurs at the point where this line crosses the origin.

positions at the transition are approximately 0.009 and 0.004, respectively. While it is very likely that the transition does occur, these quantitative conclusions should be approached with caution, as it is evident from the figure that small errors in the values of the fluid- or solid-phase chemical potentials could lead to disproportionately large errors in the location of the transition. The extrapolation of the Mansoori *et al.* equation of state could easily introduce such errors. It should be noted that the composition-space density functional theory did not enter into this calculation.

VI. CONCLUSIONS

In this work we have applied a recently developed theory for mixtures to the study of freezing in hard sphere mixtures. The single-occupancy equation of state of the pure crystal was accurately predicted for densities below the onset of mechanical stability. Beyond this point, the theory performed less satisfactorily. At the onset of mechanical stability, the true single-occupancy equation of state is ill behaved, displaying a cusp, while the equation of state predicted by the theory continues smoothly. Given the excellent performance of the theory below the cusp density (and also in describing the fluid-phase properties[2]), we believe that the abrupt deviation of the theory from the true behavior arises primarily from errors in estimating the compositions of the appropriate (i.e., large c_0) infinitely polydisperse mixtures. As discussed in Sec. IV A, accurate evaluation of the composition at large c_0 requires very careful sampling, and probably can only be achieved by introducing constraints which govern spatial and diameter correlations. The power of the methodology is in its potential for describing a wide range of mixture behavior with a limited amount of data, and thus additional studies along these lines would certainly be worthwhile.

ACKNOWLEDGMENTS

The authors are grateful for the financial support of the U.S. Department of Energy, Office of Basic Energy Sciences, and for the allotment of supercomputer time by the John von Neumann Computer Center. D. A. K. was the holder of a Du Pont graduate fellowship and an Amoco Foundation fellowship.

APPENDIX. LEADING ASYMPTOTIC BEHAVIOR OF s_0 as $c_0 \to -1$

Here we show that the log moment s_0 diverges asymptotically as $1/(1+c_0)$ as $c_0 \to -1$. From the exact statistical mechanical expression for the composition in the semigrand ensemble,[10] we may rigorously express the composition of a mixture with a $\Delta\mu$ distribution given by Eq. (1) as

$$p(\sigma) = \frac{\sigma^{c_0} f(\sigma)}{\int_0^\infty t^{c_0} f(t)\,dt}, \tag{A1}$$

where f is a differentiable function of σ that decays exponentially as $\sigma \to \infty$. With the composition given by Eq. (A1), the log moment is

$$s_0 = \frac{\int_0^\infty \ln\sigma\, \sigma^{c_0} f(\sigma)\,d\sigma}{\int_0^\infty \sigma^{c_0} f(\sigma)\,d\sigma}. \tag{A2}$$

The behavior of s_0 as $c_0 \to -1$ may be best analyzed through an integration by parts. Application of this method to the numerator yields

$$\int_0^\infty \ln\sigma\, \sigma^{c_0} f(\sigma)\,d\sigma = -\frac{1}{1+c_0}\int_0^\infty \sigma^{c_0} f(\sigma)\,d\sigma - \frac{1}{1+c_0}\int_0^\infty \ln\sigma\, \sigma^{c_0+1} f'(\sigma)\,d\sigma, \tag{A3}$$

where the prime indicates differentiation with respect to σ. Integration by parts of the denominator produces

$$\int_0^\infty \sigma^{c_0} f(\sigma)\,d\sigma = -\frac{1}{1+c_0}\int_0^\infty \sigma^{c_0+1} f'(\sigma)\,d\sigma. \tag{A4}$$

Combination of Eqs. (A2)–(A4) finally yields the desired expression

$$s_0 = -\frac{1}{1+c_0} + \frac{\int_0^\infty \ln\sigma\, \sigma^{c_0+1} f'(\sigma)\,d\sigma}{\int_0^\infty \sigma^{c_0+1} f'(\sigma)\,d\sigma}. \tag{A5}$$

Since the second term on the right-hand side remains $O(1)$ as $c_0 \to -1$, Eq. (A5) gives directly the leading asymptotic behavior of s_0 in this limit

$$s_0 \sim -\frac{1}{1+c_0} \quad c_0 \to -1. \tag{A6}$$

We may use the composition given by Eqs. (5) to determine the limiting value of $s_0^* + 1/(1+c_0)$ as $c_0 \to -1$. In this limit, the composition is well approximated by

$$p(\sigma) = \frac{\sigma^{c_0} \exp(b_{31}\sigma^3)}{\int_0^\infty t^{c_0} \exp(b_{31} t^3)\,dt}, \tag{A7}$$

where b_{31} is given in Table I. The log moment follows directly

$$s_0^* + \frac{1}{1+c_0} = \tfrac{1}{3}\left[\Psi(Z) - \ln(-b_{31}Z)\right], \tag{A8}$$

where the group $(4+c_0)/3$ has been expressed as the compressibility factor Z. Also, $\Psi(t)$ is the psi function, defined as $d[\ln\Gamma(t)]/dt$, where $\Gamma(t)$ is the Gamma function. For

$c_0 = -1, Z = 1$ and the right-hand side of Eq. (A8) is equal to -0.0582.

[1]D. A. Kofke and E. D. Glandt, J. Chem. Phys. **90**, 439 (1989).
[2]D. A. Kofke and E. D. Glandt, J. Chem. Phys. **92**, 658 (1990).
[3]W. G. Hoover and F. H. Ree, J. Chem. Phys. **47**, 4873 (1967); W. G. Hoover and F. H. Ree, *ibid.* **49**, 3609 (1968).
[4]P. Pieranski, Contemp. Phys. **24**, 25 (1983).
[5]J. J. Vieceli and H. Reiss, J. Stat. Phys. **7**, 143 (1973).
[6]T. V. Ramakrishnan and M. Yussouff, Phys. Rev. B **19**, 2775 (1979); B. B. Laird, J. D. McCoy, and A. D. J. Haymet, J. Chem. Phys. **87**, 5449 (1987); A. D. J. Haymet, Ann. Rev. Phys. Chem. **38**, 89 (1987); for an introductory review see, A. D. J. Haymet, Science **236**, 1076 (1987).
[7]S. J. Smithline and A. D. J. Haymet, J. Chem. Phys. **86**, 6486 (1987).
[8]R. McRae and A. D. J. Haymet, J. Chem., Phys. **88**, 1114 (1987).
[9]J. G. Briano and E. D. Glandt, Fluid Phase Equil. **14**, 91 (1983); J. G. Briano and E. D. Glandt, J. Chem. Phys. **80**, 3336 (1984); J. G. Briano, Ph. D. thesis, University of Pennsylvania, 1983.
[10]D. A. Kofke, Ph. D. thesis, University of Pennsylvania, 1988.
[11]H. Reiss, H. L. Frisch, and J. L. Lebowitz, J. Chem. Phys. **31**, 369 (1959).
[12]N. F. Carnahan and K. E. Starling, J. Chem. Phys. **51**, 635 (1969).
[13]G. A. Mansoori, N. F. Carnahan, K. E. Starling, and T. W. Leland, Jr., J. Chem. Phys. **54**, 1523, (1971).
[14]If Δx, Δy, and Δz measure the displacement of the center of a sphere from the center of its fcc cell in the x, y, and z directions, respectively, then the center of the sphere is within the cell if all of the following conditions hold: $|\Delta x| + |\Delta y| < D$; $|\Delta x| + |\Delta z| < D$; and $|\Delta y| + |\Delta z| < D$; where D is $\sqrt{2}\times$one-half the nearest-neighbor separation, and $||$ indicates the absolute value. This result is derived in Ref. 10.
[15]W. W. Wood, J. Chem. Phys. **48**, 415 (1968).
[16]J. Kolafa, Mol. Phys. **59**, 1035 (1986).
[17]K. Hall, J. Chem. Phys. **57**, 2252 (1972).